Journal of Biogeography, **27**, 57–69

Characterization of the spatio-temporal patterns of global fire activity using satellite imagery for the period April 1992 to March 1993

Edward Dwyer[1]*, José M. C. Pereira[2], Jean-Marie Grégoire[1] and Carlos C. DaCamara[3]
[1]*Global Vegetation Monitoring Unit, TP 440, Space Applications Institute, Joint Research Centre, European Commission, 21020 Ispra, Italy,* [2]*Departamento de Engenharia Florestal, Instituto Superior de Agronomia, Universidade Técnica de Lisboa, Tapada da Ajuda, 1399 Lisboa Codex, Portugal,* [3]*Departamento de Fisica, Universidade de Lisboa, Campo Grande, Ed. C1, Piso 4, P-1700 Lisboa, Portugal*

Abstract

Aim This paper describes the characteristics of the spatio-temporal distribution of vegetation fires as detected from satellite data for the 12 months April 1992 to March 1993.

Location Fires are detected daily at a spatial resolution of 1 km for all land areas of the globe.

Methods From the fire location information a daily gridded product at 0.5° by 0.5° has been constructed. Two methods of characterizing the spatio-temporal pattern of vegetation fires are discussed. The first applies empirical orthogonal function analysis to the monthly series of gridded data. The second approach defines and extracts a number of spatial and temporal parameters from the gridded product. The descriptive parameters extracted are used in a cluster analysis in order to group cells with similar characteristics into a small number of classes.

Results Using daily global satellite observations, it is possible to characterize the spatial and temporal variability in fire activity. Most of this variability is within the tropical belt, where the majority of fire activity is concentrated, nonetheless fire was also detected in temperate and boreal regions. The period in which fire occurred varied from region to region. Parameterization provided a very synthetic view of this variability facilitating regional intercomparison. Clustering identifies five classes of fire activity, each of which can be associated with particular climatic conditions, vegetation types and land-use.

Main conclusions Global monitoring of vegetation fire from satellite is possible. The analysis provides a coherent, consistent and synoptic view of global fire activty with one data set. The type of information extracted can be of use in global atmospheric chemistry modelling and for studying the role of fire in relation to global change issues.

Keywords
Vegetation fire, global fire patterns, remote sensing of fire, empirical orthogonal functions

INTRODUCTION

Fire has been very much in the public eye recently with images of out of control forest burning in Indonesia and Brazil, fires threatening cities in the United States, Europe and Australia and whole regions of Southeast Asia engulfed in smog. Fires caused by lightning in boreal regions of North America and Russia are responsible for up to 80% of the area burned (Stocks, 1992). However, from a global perspective, the majority of fires are man-made. They are used for many reasons such as grassland management, burning of crop residues, elimination of disease bearing insects and snakes, hunting and land clearance (Andreae, 1992). Fires are also caused by negligence and their ability to get out of control can be aided by climatic conditions.

Irrespective of the causes of fire, burning leads to the emission

Correspondence: J.-M. Grégoire, Global Vegetation Monitoring Unit, TP 440, Space Applications Institute, Joint Research Centre, European Commission, 21020 Ispra, Italy
*Now at SARMAP S.A. 6980 Croglio, Ticino, Switzerland

of vast amounts of gaseous and particulate matter (Crutzen & Andreae, 1990). It is estimated that up to 40% of CO_2 production due to human activities may be due to biomass burning (Levine, 1996). The emissions of CO_2 in addition to a range of other gases such as CO, CH_4 and NO_x are of interest in atmospheric chemistry modelling to determine the contribution of vegetation fire to climate change through forcing of the earth's radiation budget. Fire is an ecosystem disturbance. It partially or completely removes the vegetation layer. This can be very dramatic as in the burning of forest or more subtle as in the burning of bush and grasslands. Timing and severity of fire can affect succession, favouring those species which have developed an adaptation to fire. It can affect plant nutrition in a variety of ways. The ash can provide a sudden pulse of nutrients to the soil but conversely the burned surface is more sensitive to nutrient leaching, soil erosion and changes in the hydrological cycle than the vegetated surface (Menaut *et al*., 1993).

To improve understanding of the role of vegetation fire emissions in atmospheric chemistry and fire itself as an ecosystem disturbance there has been a request for information on fire from the international science community. This has been focused through a number of core projects of the International Geosphere Biosphere Programme (IGBP) such as the International Global Atmospheric Chemistry Project (IGAC) and the Global Change and Terrestrial Ecosystems (GCTE) project (IGBP, 1994). Their information requirements include global fire distribution, timing, extent, severity and return frequency. Other groups which require fire related data include international organizations involved in environmental policy and management and national organizations with land management mandates.

The term *fire regime* is used to describe a collection of attributes pertinent to fires in a given ecosystem or region. Usually included are fire frequency ($1/n$ years), intensity, date of occurrence and fuels involved. Some aspects of fire regimes are known and have been documented for many global ecosystems (Stocks, 1992; Goldammer, 1993; Trabaud *et al*., 1993). However, their characterization is rather generalized and is usually described in terms of probability of occurrence or fire frequency (Malingreau & Grégoire, 1996). We are still unable to answer the simple question: where and when do fires occur? We have lacked the spatial and temporal detail needed to help meet the requirements for global change studies. Since the early 1980s satellite data have been used to determine the spatial and temporal location of fires. A wide range of optical and infra-red sensors have been employed to detect active fires and burned surfaces at different spatial resolutions, for different times of the day, at local, regional and continental scale and for different time periods. Good reviews of the different approaches are given in Robinson (1991) and Eva & Lambin (1998).

Although these data sets are valuable, they are not appropriate for building a global database of fire occurrence due to the heterogeneity of the source data and processing methods. This lack of coherent, consistent and systematic information on vegetation fire led the IGBP to propose and support the development of a satellite based, global fire product using one data source for a relatively extended period of time, processed using a single methodology based on an algorithm accepted by the international community of experts in remote sensing of vegetation fire (IGBP, 1997; Stroppiana *et al*., 1999)

Global, time-series data sets are large and complex by their nature. The information must be summarized in a quantitative and objective manner which goes beyond simply displaying large quantities of data. Analysis methods are only now being developed. Davis *et al*. (1991) pointed to the lack of quantitative analysis techniques for multitemporal imagery while Piwowar *et al*. (1998) called attention to the fact that little development had occurred on exploring methods to highlight space-time relations in data.

The objective of this paper is to describe the characteristics of the spatio-temporal distribution of vegetation fires as detected from satellite data for the 12 months from April 1992 to March 1993. This is achieved by using analysis techniques which highlight the spatial and temporal variability and present it in a small number of new variables. The patterns of fire distribution identified, using two different techniques, are described and their significance in relation to climate and vegetation distributions are discussed.

DATA AND METHODS

The global satellite fire data set

The geographical positions of those pixels in which fires were detected (fire pixels) were determined from a global 1 km Advanced Very High Resolution Radiometer (AVHRR) data set for each day in the 21-month period from April 1992 to December 1993 (Stroppiana *et al*., 1999). This data set is the first of its kind to give a global picture of vegetation fire, using a single data source and a single fire detection algorithm, which leads to an internally consistent data product (Dwyer *et al*., 1998). However, as with any remotely sensed data product there are limitations. The product represents a sample of the total fire activity which took place during the period as only those fires which were active during the time of satellite overpass, in the early afternoon, were recorded. For some regions of the tropics this coincides with the time of peak fire activity (Eva & Lambin, 1998). False detection can occur due to the algorithm considering certain ground features, such as hot soil or sun-glint from water as fire events. An evaluation of various fire detection algorithms for global applications is given in Giglio *et al*. (1999) and the one used to produce the data set discussed here is described in detail in Flasse & Ceccato (1996).

Each fire pixel detected represents a point event, at a spatial resolution of 1 km, in space and time. In order to characterize spatial patterns for the globe it was first necessary to aggregate fire counts for larger spatial units. We chose to work with only the first 12 months of data as this represents one complete fire cycle or season for the whole globe. The fire pixels were aggregated into cells of fire pixel counts for each day at a resolution of 0.5° by 0.5° for the whole globe. The gridding procedure produces a pseudo-continuous surface and a data set of reasonable dimensions for further processing and analysis.

Choosing the cell size is a nontrivial problem. Surface processes tend to be scale dependent. A phenomenon may appear homogenous at one spatial scale but heterogeneous at another (Davis *et al.*, 1991). The cell size used here was considered appropriate for a global scale analysis as it retains major spatial variation. It is also compatible with other global scale data sets of climate parameters and vegetation type and the cell size of models used in the study of emissions and carbon cycling, thus facilitating integrated analysis.

A geographical or latitude/longitude representation does not preserve area, therefore the ground area of each aggregated grid cell (0.5° by 0.5°) decreases as a function (cosine) of latitude, with increasing distance from the Equator. This means that cell counts should not be compared without considering area. The National Oceanic Atmospheric Administration (NOAA) satellite series are polar orbiting and make approximately fourteen orbits per day. As each ground swath is a constant width of nominally 2700 km, there is increasing swath overlap as the satellite moves from the Equator towards the poles. For the purpose of this analysis, we consider the effect of reduced cell ground area to be offset by the cell being observed a number of times, therefore no area correction is made (i.e. at 60° North or South, a cell is half the area of one at the Equator, however, it is viewed twice in consecutive satellite orbits). The same fire pixel was rarely counted twice in subsequent orbits, at high latitudes. Detection depends not only on fire size and temperature, but also on satellite viewing angle (Giglio *et al.*, 1999).

Analysis techniques

In order to characterize global spatio-temporal fire patterns, two methods were explored. Empirical Orthogonal Function (EOF) analysis is useful to study phenomena which vary spatially over time as it can identify seasonal elements of change and isolated change events. It captures all modes of variability in the data, however, it can be difficult to interpret the patterns, especially in areas which contribute marginally to the variability. An alternative technique involves the extraction of predefined spatial and temporal metrics from the data set. These metrics are then used to group fire patterns in a small number of classes. It is easier than EOF analysis to interpret the fire distributions at the individual grid cell level, however, the modes of variability are restricted to only those captured by the preselected parameters.

Empirical Orthogonal Function analysis

Empirical Orthogonal Function (EOF)) analysis is a popular technique used in remote sensing studies for image enhancement and to reduce the dimensionality of multispectral data sets (Richards, 1993). It is commonly used by climatologists for the study of atmospheric circulation (Yarnal, 1993). Studies have been done using EOF analysis of multitemporal satellite imagery for land cover classification (Townshend *et al.*, 1985; Tucker *et al.*, 1985) and to detect change in time series data (Eastman & Fulk, 1993; Piwowar & LeDrew, 1996; Keiner & Yan, 1997). The method can be used to reduce the size of a data set as the bulk of the variability can be represented through a limited number of new variables or components.

The analysis involves creating a new set of variables which are a linear transformation of the input variables. The new variables or components are mutually orthogonal and therefore uncorrelated with each other. In the analysis of the multitemporal data considered here, each input variable is a two dimensional grid of fire counts accumulated over a 1-month period, therefore only variability at a monthly time scale is considered. The components are calculated by first constructing the covariance or correlation matrix of the input variables. Then the eigenvectors and corresponding eigenvalues of this matrix are extracted. The EOFs are calculated by multiplying the matrix of input variables by the transpose of the eigenvector matrix. A full mathematical treatment of the method is found in many texts (Johnston, 1978; Gonzalez & Wintz, 1987; Richards, 1993).

In the analysis of time series data of a single environmental variable, it has been observed that the first EOF indicates the characteristic value or 'typical' condition of that variable; the second identifies the main seasonal evolution in the variable, while the higher components represent increasingly local variations and anomalies (Eastman & Fulk, 1993; Piwowar & LeDrew, 1996). This is not an intrinsic property of EOF analysis. The distribution of the variability in that order could be considered coincidental. By definition, the first EOF contains most of the variation found in the original data set, subsequent components contain progressively decreasing amounts of variance. There are three outputs from the analysis which are of interest. The component *loadings* show the strength of the relationship between each input variable and the corresponding component. The component *scores* are the values for each observation on the new variables or components, thus if an observation has high values for the variables with large loadings on the component, then it should have a high score on the component. The *eigenvalue* is the sum of the squared loadings for each input variable and indicates the total variance accounted for by that component.

If there is significant correlation between the input variables, then in general only the first few components are retained from the analysis, as they contain most of the variance in the data set. The higher order components contain progressively less information from the source data and in certain circumstances they can be considered as noise. The decision as to the number of components to keep is somewhat subjective. Although statistical tests can be used to determine a cut-off point, these are considered of limited use in practice (Davis, 1973). It is more appropriate to keep those components which can be interpreted in relation to the phenomenon being studied (Piwowar & LeDrew, 1996). There has been some debate as to whether standardized or nonstandardized components should be calculated when using multitemporal data (Singh & Harrison, 1985; Fung & LeDrew, 1987; Piwowar & LeDrew, 1996). In a nonstandardized analysis the eigenvectors and hence the loadings are calculated from the covariance matrix of the input variables. Here, each input variable corresponds to the matrix of monthly fire pixel counts. Those which have a higher variance will have a greater influence on the generated EOFs in a nonstandardized analysis. In a standardized analysis the components are calculated from the correlation matrix. This has the effect of giving each input variable a mean of zero and a standard deviation of one. Hence, all variables are of equal importance in the analysis. In this data set the standard deviation of the fire counts varies by a factor of 2 over the 12 months, therefore in order to minimize the effect of those months showing a large variability we have calculated the standardized components.

Spatial and temporal descriptors

Another approach to capturing space-time variability relies on the explicit extraction of spatial and temporal variables or metrics from the data being studied. These variables can then be integrated into a single classification scheme which characterizes variability in a number of groups or classes. Clustering and classification is a powerful method for capturing and simplifying the heterogeneity in a data set and expressing it as a small umber of classes, which are often easier to interpret than the original data. These techniques have been used to determine different land cover types for global mapping by using remotely sensed satellite data (Lloyd, 1990; DeFries *et al.*, 1995). Several approaches to characterizing fire patterns in terms of their spatial and temporal aspects have been proposed. Goldammer (1993) defined seven different regimes for tropical and subtropical regions based on fire frequency or return interval, fire intensity (e.g. surface *v.* crown fire) and impact on soil. Christensen (1993) defines the components of a fire regime as intensity, frequency, spatial extent, seasonality and predictability, while Grégoire (1993) defines regime for tropical regions in terms of the temporal distribution of fire events in a given geographical area throughout the dry season.

The parameters which can be extracted from the data set described earlier incorporate many of these concepts.

Spatial descriptors

Fire number: for each 0.5° by 0.5° grid cell the total number of fire pixels detected in the year was calculated;
Fire agglomeration size: this is a measure of the degree to which fire pixels are clustered within each grid cell. During the fire detection process fire pixels are geolocated on a latitude/longitude grid at 0.01° resolution, but adjacent image pixels may not be projected to adjacent positions in the latitude/longitude frame. This is due to the variable pixel size in both along track and across track directions (Frulla *et al.*, 1995). By accumulating the projected data into cells of 0.02° by 0.02° this effect can be mitigated to some extent. Many fire pixels that were adjacent in the image frame are now adjacent in the 0.02° by 0.02° lat/lon gridded data. Then for each day within each half degree cell, the average agglomeration size was calculated using simple neighbourhood analysis as shown in Fig. 1.

Temporal descriptors

The period of the year in which burning occurs in a given region is often referred to as the fire season. Four descriptors of the season have been extracted for each grid cell and are defined as follows.
Season start: this was defined as the time when 10% of all fire pixels in the year were detected. This threshold was chosen in order to reduce the effect of occasional or very low levels of fire activity which may take place throughout the year;
Season end: this was defined as the time when 90% of all fire pixels were detected. Again this threshold was imposed in order to filter out very low levels of fire activity;
Mid season: this was defined as the time when 50% of all fire pixels were detected. This is not the same as the time of peak fire occurrence, which can be at any time within the fire season;
Season duration: time between the start and end of the season.

Although the concept of season may not be appropriate for cells containing only one fire pixel or those in which burning continues all year, the above definitions allow a value to be assigned to each cell. In order to calculate the descriptors for all grid cells, fire occurrence was considered to be identical for the year preceding and the year subsequent to that analysed. This is not the case in reality, but was a necessary assumption given the lack of a multiannual data set.

Of the six parameters extracted, both spatial descriptors and one temporal descriptor (season duration) were chosen for input to a clustering algorithm. The other temporal descriptors were not used in the classification as they are dependent on northern/southern hemisphere seasonal effects. The resulting classification should therefore be more easy to compare across geographical regions.

Agglomeration sizes can and do change over the duration of the fire season, but to simplify the classification one period was selected for all grid cells. This was the average agglomeration size during 10 days centred on the mid season. An average over the complete fire season resulted in all cells having a small agglomeration size. The three parameters, which are not significantly spatially correlated, were standardized and input to the ISODATA clustering algorithm which produced a series of classes that group cells exhibiting similar spatial and temporal attributes. By examining the cluster signatures and merging similar cluster groupings, five distinct classes were selected.

RESULTS

Empirical Orthogonal Function analysis

Table 1 shows the eigenvalues and the percentage of the total variance explained by each of the components extracted. Here we present the first four components which account for 73% of the variability and can be readily interpreted. Using these four components the original twelve monthly fire count maps were reconstructed. A visual interpretation indicated that all major spatial and temporal features were retained, although some local variability was lost. For each component the loadings plot is given (Fig. 2) with the corresponding scores for all cells presented as an image (Fig. 3). A month which shows a strong positive or negative loading or correlation on a given component indicates that the month contains a spatial pattern which has close similarities with the one shown in the component. The

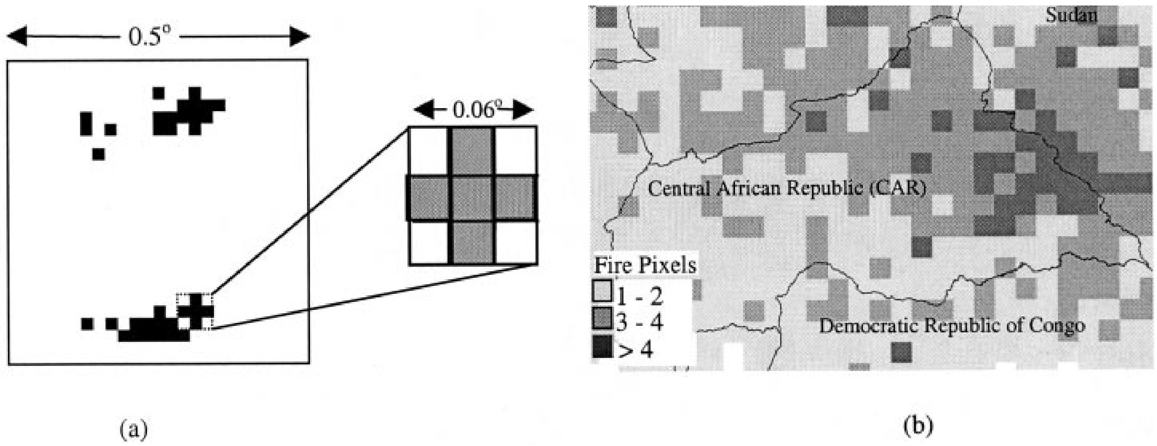

Figure 1 (a) Within each 0.5° by 0.5° cell, the fire pixels are accumulated in 0.02° by 0.02° cells. The agglomeration size is calculated as the total number of fire pixels in this smaller cell and its immediate eight neighbours (a 0.06° by 0.06° area). This procedure is repeated for each fire pixel in the 0.5° by 0.5° cell. To calculate the agglomeration size for 0.5° by 0.5° cell edge pixels the neighbouring cells' pixels are included. The average agglomeration size is then calculated from these individual values for each 0.5° by 0.5° grid cell for each day. (b) Example of the average fire agglomeration size in cells of 0.5° by 0.5° during the mid fire season 10 day period. Large savanna fires in the sparsely populated areas on the border between CAR and Sudan are often set by hunters and left to burn uncontrolled, while in the west of CAR fires are used for agricultural purposes and are therefore controlled and smaller. The three classes indicate the number of fire pixels detected in each 0.06° by 0.06° area averaged for the whole 0.5° by 0.5° cell.

Table 1 The eigenvalues and the percentage of the total variation explained by each of the twelve components of the empirical orthogonal function analysis.

Component	Eigenvalue	% variance	% Accumulated variance
1	3.4	28.3	28.3
2	2.4	20.0	48.3
3	1.8	15.0	63.3
4	1.2	10.0	73.3
5	0.9	7.5	80.8
6	0.6	5.0	85.8
7	0.5	4.2	90.0
8	0.3	2.5	92.5
9	0.3	2.5	95.0
10	0.2	1.7	96.7
11	0.2	1.7	98.4
12	0.2	1.6	100.0

sign of the loadings and hence of the score images allows the geographical location of the patterns to be identified.

EOF 1, by definition, accounts for the largest proportion of the variance in the data set. The loadings plot (Fig. 2(a)) is almost flat, which indicates that, by and large, the spatial pattern of EOF 1 is representative of fire activity during the whole year. This spatial pattern, shown in Fig. 3(a), indicates that the highest score values coincide with the areas of highest fire number, the location of which is almost completely within the tropical belt. This component accounts for slightly less than 30% of the total variability in the data set, hence further components must be interpreted in order to explain more fully the fire distributions.

The second component or EOF exhibits an accentuated

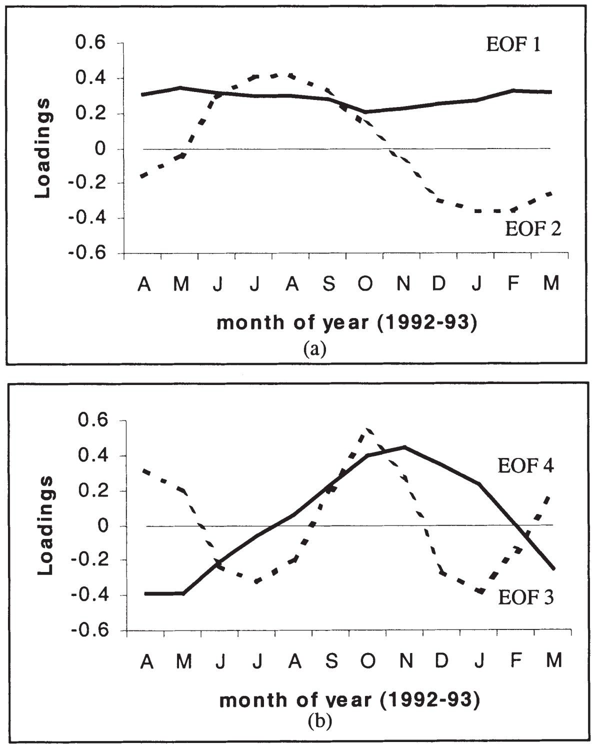

Figure 2 The eigenvector loadings for the first four empirical orthogonal functions derived from the global active fire distributions for the period April 1992 to March 1993. EOF 1, characteristic fire activity; EOF 2, timing of northern/southern hemisphere tropical fire season; EOF 3, spring/autumn fire season; EOF 4, semi-annual cycle.

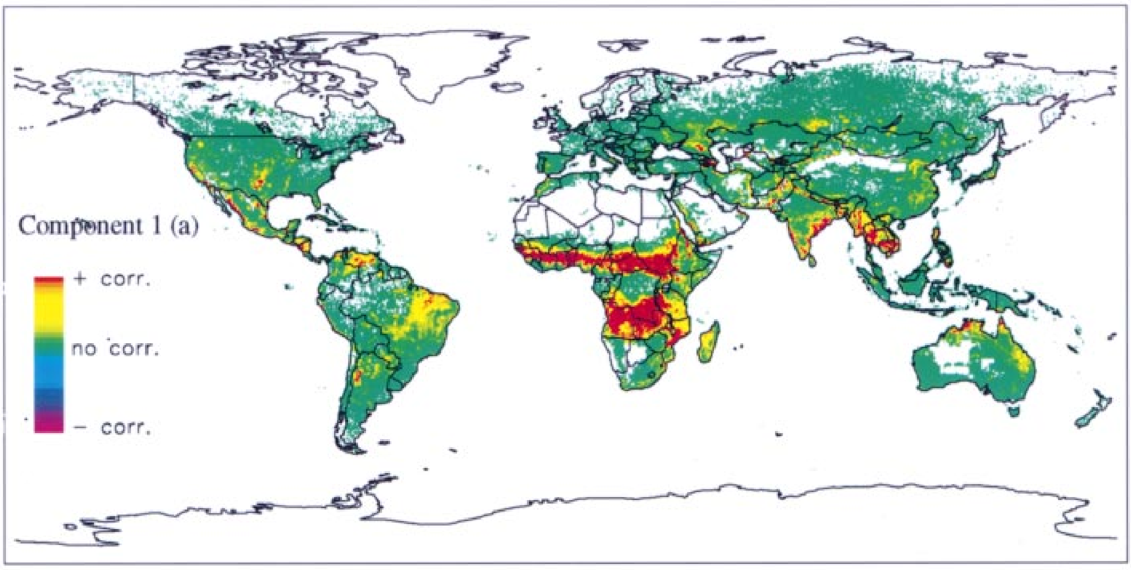

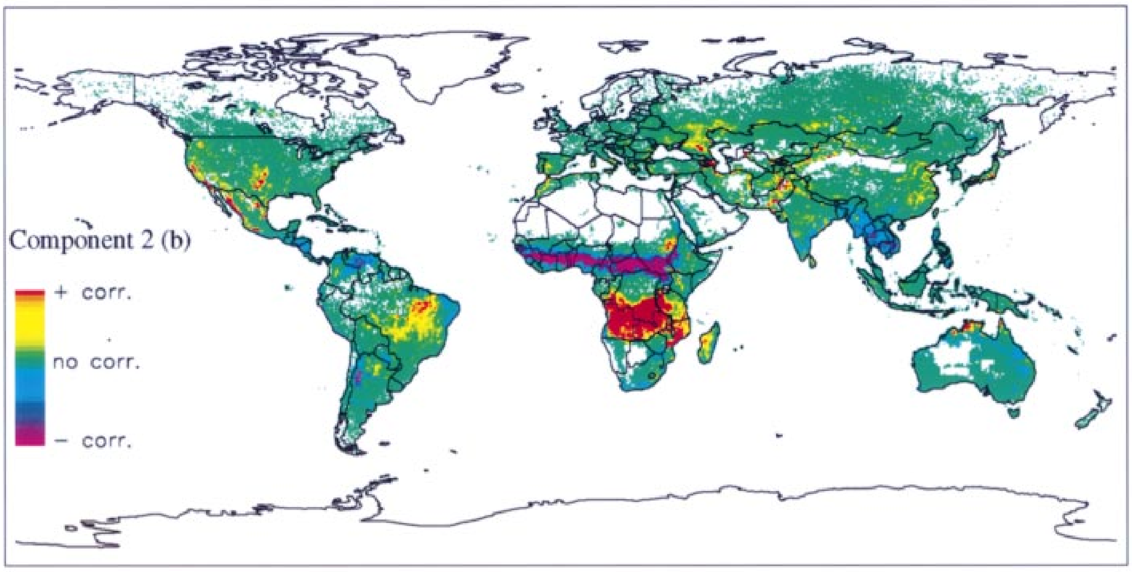

seasonal variability (as can be seen in the loadings plot, Fig. 2 (a)). The high positive correlations from June to September correspond to fire activity in the tropical belt of the southern hemisphere as can be seen in the scores image, Fig. 3(b). The cross over point in November, Fig. 2(a), is when minimum global fire activity occurs and the strong negative correlation values in January and February are associated with high fire activity in the northern tropics, mainly in Africa. The bimodal nature of the loadings plot corresponds, to some extent, to the yearly change of seasons.

Component 3 also shows a strong annual cycle, but it highlights fire activity occurring during the Spring and Autumn. High positive correlations in October and November, Fig. 2 (b), are associated with fire activity at the beginning of the dry season in Africa, north of the Equator and with the end of the fire season in south-east Africa, Brazil and northern Australia, Fig. 3(c). The negative correlation values correspond to high fire activity in Southeast Asia and India as well as parts of Central America and South America, north of the Equator, in April and May. An interesting detail highlighted in this component is the high negative scores seen in Africa in the west of the Republic of Guinea and in southern Sudan, compared with the positive values for the rest of the region. In contrast to surrounding areas, rainfall amounts were less

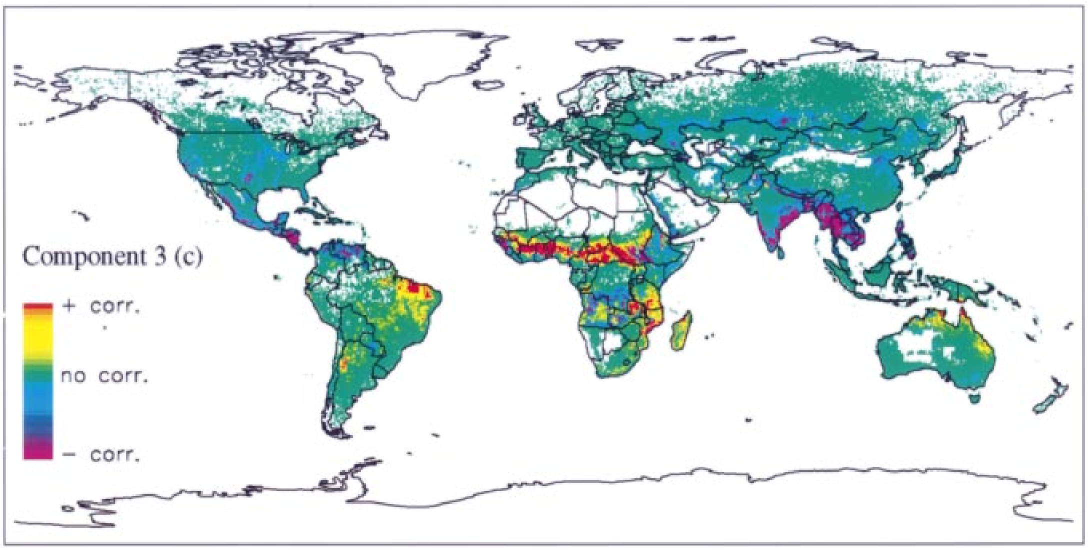

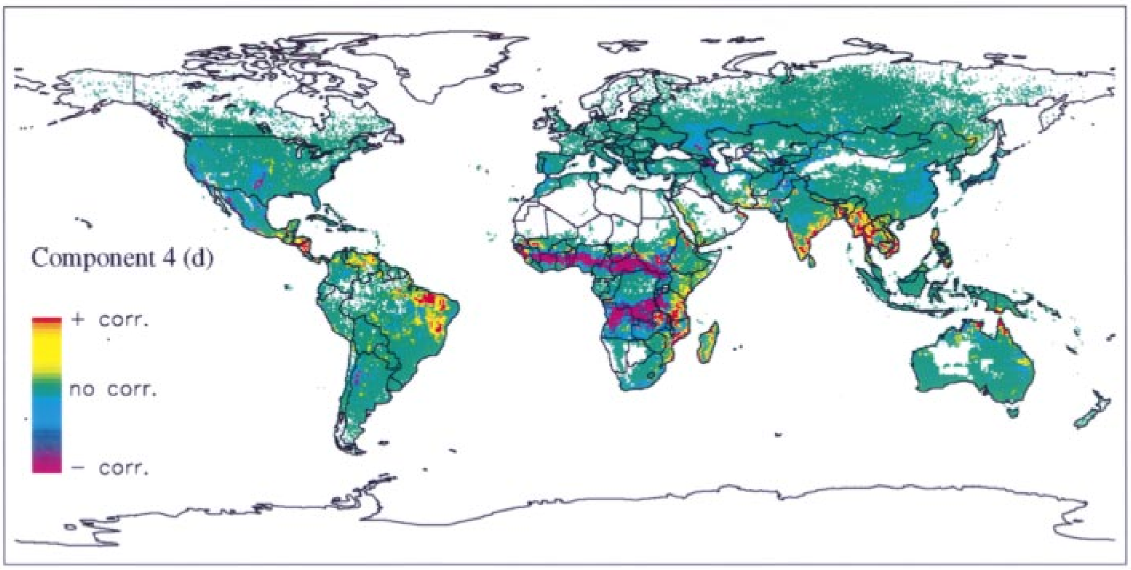

Figure 3 The scores for the first four empirical orthogonal functions derived from the twelve months of active fire position data. To enhance visualization, the top (and bottom for components 2, 3 and 4) 5% of values have been saturated, i.e. the highest 5% of data cells take on the most positive correlation colour, while the lowest 5% take on the most negative correlation colour.
(a) Characteristic fire activity, (b) timing of northern/southern hemisphere tropical fire season, (c) spring/autumn fire season, (d) semi-annual cycle.

than normal in western Guinea in April and May 1992, which may have resulted in an extended fire season. The area in southern Sudan is centred on the Jonglie marsh and it is known that fishermen burn off reeds and grasses in the late dry season to improve accessibility (Mr M. Lock, personal communication).

Component 4 shows a semiannual cycle in the loadings, Fig. 2 (b). Examination of the scores image, Fig. 3 (d), indicates that the positive values seen in April and May correspond to high fire activity in mainland Southeast Asia, as already noted in component 2, while the negative values from June to August coincide with high fire activity in south-west Africa. The peak in the loadings plot in October corresponds to an area of burning in north-east Brazil, south-east Africa and part of the Northern Territory in Australia. The negative values in December and January correspond to a high level of burning in subsaharan Africa, north of the Equator.

The higher components account for progressively decreasing amounts of variation, representing local variations in fire

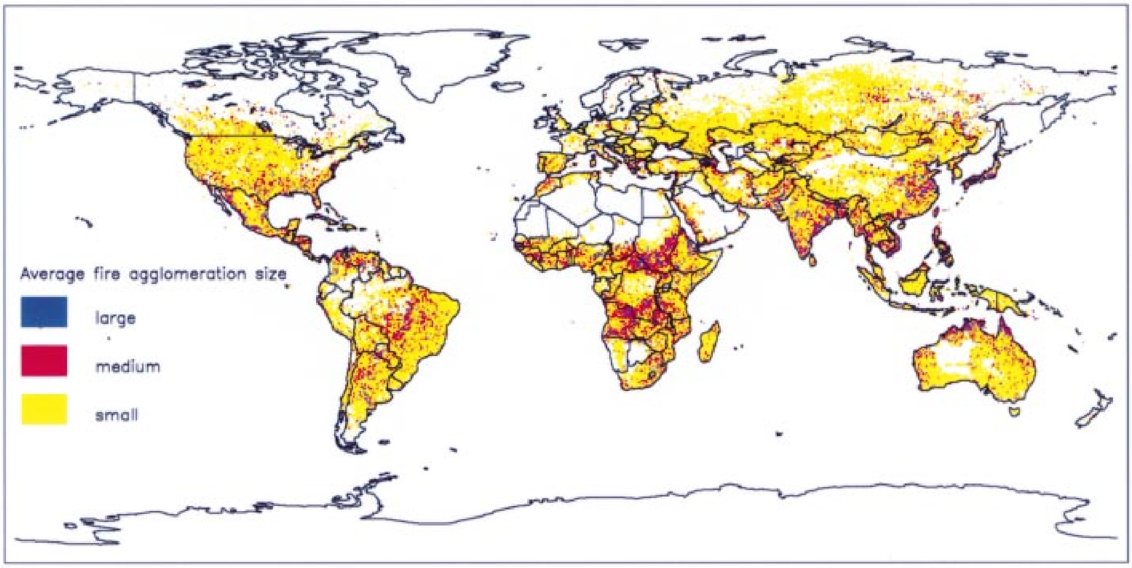

Figure 4 The average agglomeration size in each 0.5° by 0.5° cell during the 10 day period centred on the mid fire season, for the year April 1992 to March 1993. (Small, 1–2 fire pixels; medium, 3–4; large ≤ 4).

activity and significant regional patterns are difficult to determine.

The EOF analysis has been an effective method for concentrating the majority of global and regional variability in fire distributions in just four new variables. In addition, the modes of variability described are not correllated. The component score plots display and highlight the spatial pattern of fire activity. Not only is the well documented shift of burning with the dry season in the Tropics from the northern to the southern hemispheres revealed (EOF 2), but the difference in the timing of the fire season between the northern tropical belt of Africa and that of peninsular Southeast Asia, India and Central America is also clearly evident (EOF 3). A drawback of the technique is that it is difficult to interpret, in a geophysical sense, all patterns unambiguously. In addition, little information on the temporal dynamics of the fire season is gained for those regions which make a small contribution to overall variability. An alternative method is used to address these shortcomings.

Parameter extraction

A total of six parameters were extracted from the 0.5° by 0.5° gridded data set, two based on the spatial and four on the temporal distributions of the fire pixels.

The spatial pattern of the accumulated number of fire pixels for the 12-month period is very similar to the first EOF, which showed fires in almost all regions of the world but with a high concentration of events in the tropics.

Figure 4 shows the average fire agglomeration size for the whole globe during the 10-day period centred on the mid season. A comparison of the spatial distribution of average fire agglomeration sizes during the months representing the start, mid and end of season shows that, in general, in tropical regions the number of cells containing larger agglomerations increases from the start to the middle of the season and then decreases again towards the end of the season. The size of fire agglomerations is an indicator of land-use and fire practices. Large fire agglomerations were consistently found on the border between Sudan and the Central African Republic, Fig. 1(b). This is a sparsely populated savanna region where many fires are set by hunters and then left to burn uncontrolled (Eva *et al.*, 1998). On the contrary, in the west of the Central African Republic, fire agglomerations get smaller from the middle to the end of the season. Mid season fires are associated with grassland management, while late season fires are used in preparation of croplands before the first rains and are generally smaller. One notable exception to this pattern is seen in India and Southeast Asia where the number of bigger agglomerations continues to increase towards the end of the fire season. At least in Southeast Asia, the increase may be due to shifting cultivation within fragmented forest. The most efficient burns are achieved towards the end of the dry season after prolonged drying of felled vegetation (Jones, 1997). In eastern Siberia and parts of Ontario and Manitoba in Canada many large agglomerations are seen. Here many of the biggest fires occur in sparsely populated regions and are often allowed to burn out naturally (Stocks *et al.*, 1996).

Figure 5 shows the month corresponding to the middle of the fire season for every grid cell containing one or more fire pixels. Equivalent plots can be constructed for the start and end of season. Although the EOF analysis revealed the temporal trends in burning, in particular for tropical areas where there was a high number of fires, little information was available for those cells with few fires. The figure shows that the middle of the burning season runs from May to August in most regions of the northern hemisphere's temperate and boreal biomes, while in the temperate regions of the southern hemisphere, the mid season is from December to March. The timing and

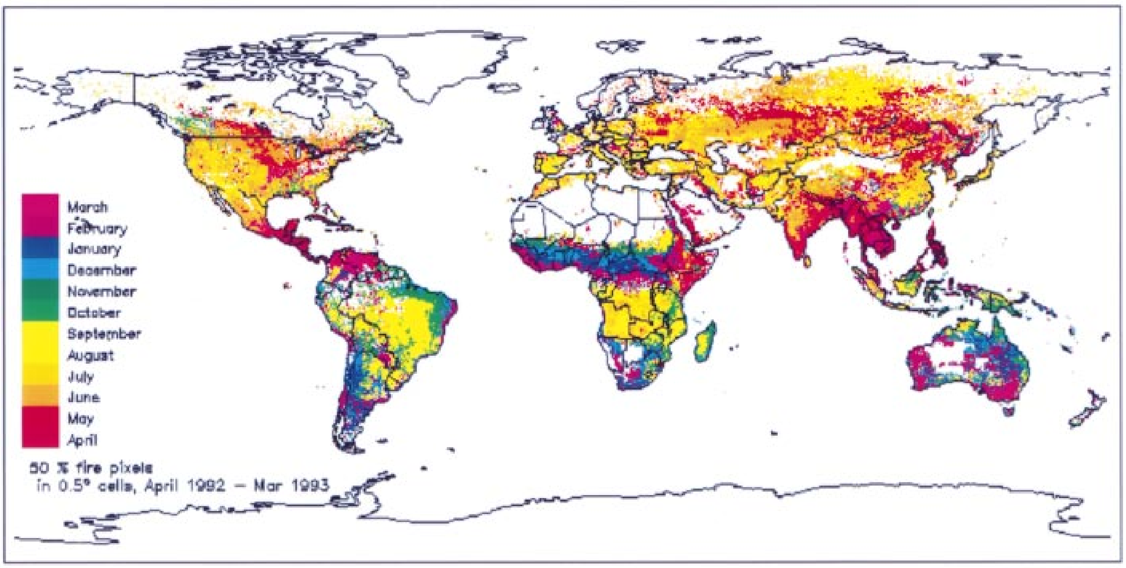

Figure 5 For each 0.5° by 0.5° cell the month of the mid fire season is shown. This is independent of the number of fire pixels detected in a cell.

Table 2 The mean value of the three input variables is shown for the five classes defined in the cluster analysis using *a-priori* defined parameters. Also shown in the percentage of cells in each class.

Class	Number of fire pixels (mean)	Duration (months) (mean)	Agglomeration size (pixels) (mean)	% in class
1	31	1.4	1.2	32
2	101	3.4	1.2	24
3	94	6.1	1.4	23
4	220	3.0	3.7	15
5	1211	3.5	2.6	6

duration of the fire season are important parameters used in determining the amount of trace gases and aerosol particles emitted from burning biomass. Fire season duration, which is calculated from the time of observation of the first and last fire events during the year, should not be confused with the period of fire risk. For example in northern Siberia, most fire cells show a fire season duration of one month. However, on average, there is a high fire risk for three to four months in this region (Stocks *et al*., 1996). In temperate and tropical regions the fire season duration was three to four months while in more arid regions, such as the horn of Africa, interior Australia and central India the fire season was seen to last six months or more.

Classification

An automatic clustering algorithm (ISODATA) was used to extract five classes based on the three global grids of fire number, seasonal duration and agglomeration size. Table 2 shows the mean values and the standard deviations of the three input parameters for each class, as well as the percentage of cells belonging to each class. The class characteristics can be described as follows.

Class 1: Low level of fire activity, there are few fire pixels in a cell. The fire season is short and the fire agglomerations are very small.

Class 2: Moderate level of fire activity with a moderate fire season duration, the fire agglomerations are small.

Class 3: Moderate level of fire activity, very long fire season duration. Fire agglomerations are small.

Class 4: Moderate to high level of fire activity with a moderate fire season duration. Fire agglomerations are large.

Class 5: Very high level of fire activity, moderate to long fire season duration and moderate to large fire agglomerations.

Although class 1 accounts for 32% of the cells, it only represents 6% of the total fire pixels detected. On the other hand, the 6% of cells in class 5 account for 45% of the total fire pixels detected, showing how very intense fire activity is restricted to a relatively small area.

The ability of a clustering algorithm to separate groups can be evaluated with a number of measures. One widely used method is the Jeffries-Matusita distance measure. The JM distance receives an exponentially decreasing weight with increasing separation between classes and is asymptotic towards two which indicates complete separability, while zero represents no separability (Richards, 1993). The values for all class combinations are presented in Table 3. The best separability is between classes 1 and 3, while the poorest is between classes

Table 3 The Jeffries-Matusita distance for each of the ten class combinations shows the separability between the classes constructed using the three parameters: fire count, agglomeration size and fire season duration. Zero represents no separability, two, complete separability.

Classes	JM	Classes	JM	Classes	JM
1:2	1.8	2:3	1.7	3:4	1.8
1:3	2.0	2:4	1.6	3:5	1.9
1:4	1.8	2:5	1.8	4:5	1.5
1:5	1.9				

4 and 5. This indicates that the clustering algorithm has been quite successful in identifying groups which have distinct characteristics.

Figure 6 shows the geographical distribution of the classes, with each of the 0.5° by 0.5° cells affected by fire, colour coded for the appropriate fire class. This reveals a number of interesting patterns. Boreal regions are dominated by infrequent, low levels of burning (class 1) although many fires of large agglomeration size also occur (class 4). The temperate regions of Asia, Europe and North America show moderate numbers of smaller fires with a marked fire season (class 2). Equatorial forest in both South America and Africa have a predominance of small occasional fires (class 1), although on the peripheries of the forested regions many of the other classes are evident. In the grassland areas of Brazil, fires of a marked fire season are predominant (class 2) although there is an arc of fires of large agglomeration size (class 4) close to the forest/grassland boundary. The savanna regions of Africa are dominated by very high density burning (class 5), while the arid regions in the horn of Africa indicate moderate numbers of fires occurring over a very long season (class 3). Mainland Southeast Asia and eastern India are dominated by high density burning (class 5) and a strikingly seasonal pattern of vegetation fire (class 2), while in western India and in southern China fire is of a more moderate nature, with an extended fire season (class 3). Australia and insular Southeast Asia show moderate burning levels (class 2 & 3). In the Northern Territory of Australia which is dominated by shrub land, there is a region of very high density burning and fires of large agglomeration sizes (classes 4 and 5). Other years may show different patterns of burning. In the year analysed, a low level of fire occurrence was detected in insular Southeast Asia. This would certainly not have been the case if the analysis had covered 1998.

DISCUSSION

This study has characterized global patterns of vegetation fire in a very synthetic manner while highlighting both the spatial and temporal variability of the phenomenon. It improves significantly on previous studies by presenting fire activity for the whole globe during the same time period. Although the regions in which burning was observed have been identified and reported before, this is the first time, to our knowledge, that such patterns have been detected in a single data set using the same method and described from a global perspective. The feasibility of using a single algorithm to detect fires globally has been shown. We believe that all major fire regimes, irrespective of location and timing have been detected. Of course further work must be done to determine the percentage of fires really captured, the effects of temporal sampling, cloud cover, vegetation type, etc. on the completeness of the data set. Nevertheless, this global overview should be of immense benefit for research of global biogeochemical cycles and atmospheric chemistry, as local and regional level data sets are ill-suited to such investigations (IGBP, 1992). This work confirms that most

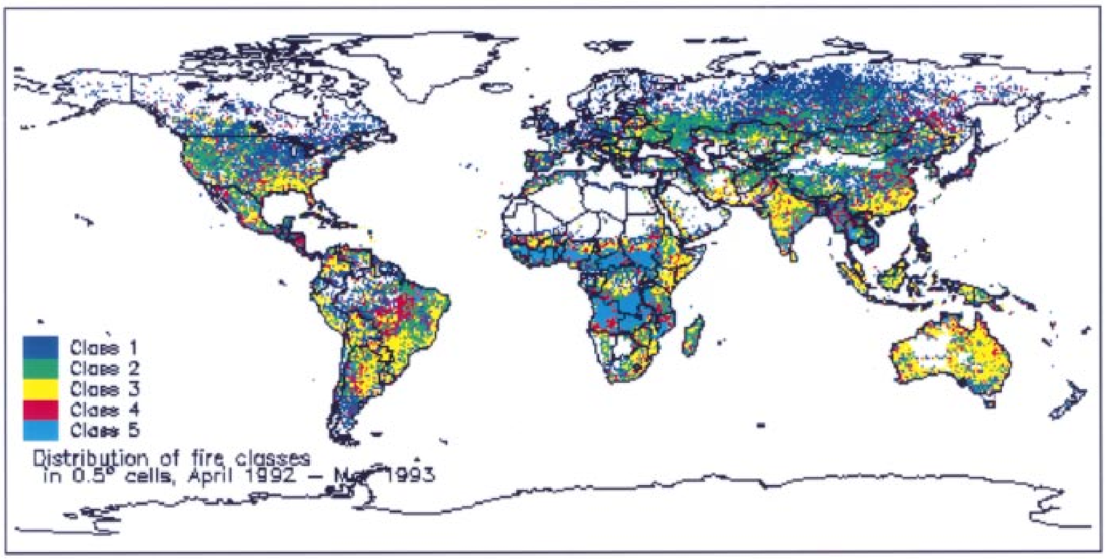

Figure 6 The spatial distribution in cells of 0.5° by 0.5° of the five fire classes defined using the cluster analysis of fire count, agglomeration size and fire season duration.

fire activity occurs in the tropics (Crutzen & Andreae, 1990; Andreae, 1992), and identifies the most significant spatial and temporal variability across this belt.

Both the EOF approach and the extraction of temporal parameters summarize temporal variability very effectively. The strongest temporal variability in biomass burning is that associated with the movement of the dry season in the tropics from the northern to the southern hemisphere, as evidenced in the second EOF. In addition, there is a very clear separation in time between burning in Africa and that in Central America and southern Asia, the latter occurring most intensely in April and May, when in Africa it is a transition period between burning in the northern and southern hemispheres. The timing of the burning season conflicts to some extent with those studies which have used the concentration of surface ozone as a proxy for the presence of biomass burning. For Africa, during the year studied here, most fires were observed a couple of months earlier than those reported by Hao & Liu (1994) for the northern hemisphere and also earlier than those reported by Delmas *et al.* (1992) and Hao & Liu (1994) for the southern hemisphere. The timing of the fire season here is more in line with that determined from previous satellite observations (Cahoon *et al.*, 1992; Koffi *et al.*, 1996). Kim & Newchurch (1998) associate high levels of lower-tropospheric ozone, in the period July to September, averaged over the period 1979–93, in western New Guinea, with biomass burning in the western part of the island. This conflicts, to some extent, with our observations, where the peak fire season was from September to November with most activity concentrated in the southern part of the island. It is possible that the dry season was later or longer than usual in 1992, however, the use of satellite observations of fire activity can certainly improve on the use of measurements of other variables to infer burning.

In addition to highlighting the spatial and temporal distributions in tropical burning, the burning patterns in temperate and boreal regions are also captured. Monitoring of fire in boreal regions is important due to the significant role that boreal forest plays in global carbon cycling. Fire in such ecosystems has huge direct and indirect impacts on the carbon pool (French *et al.*, 1996). The temperate and boreal regions contribute significantly to the number of fires observed in the period May to August, which coincides with the northern hemisphere's summer. The classification (Fig. 6) shows fire activity in many parts of the United States. In Eurasia a band of fire activity stretches from the Black sea to Lake Baikal, while in the more northern regions of Siberia and North America, large fire agglomerations can be seen.

Some problems remain with the automatic fire detection algorithm (Stroppiana *et al.*, 1999). Many false fires were detected in the north-western part of Argentina on the border with Chile. In semidesert areas of the Arabian peninsula, southern Africa and Australia, we also observe unexpected fire activity. These detections are most likely associated with areas of hot soil or bright surfaces. The radiative response from the sensor's perspective is the same as that of a fire and the algorithm used is not sufficiently sophisticated to distinguish between this and actual fire events. Another problem is associated with sun glint from temporary water bodies. At certain sun-target-sensor angles, there is specular reflection into the sensor optics. The values recorded are then interpreted by the fire detection algorithm as 'hot spots' which leads to false fire detection. Although burning of crop residues in the field is common in south-eastern China, and the spatial location of the fire activity coincides with that of estimated residue emissions (Zhuang *et al.*, 1996) we believe that some of the very large fire agglomerations seen here are associated with sun glint from flooded paddies.

The EOF analysis is ideal for capturing and separating all modes of variability within a data set and here it has been particularly effective in highlighting the variation in timing of the fire season across the tropical belt. Conversely, the parameter extraction and classification technique limits the range of variability described to those metrics chosen, however, the spatial and temporal patterns are easier to interpret geophysically. The classification method will be considered in the following discussion.

Figure 6 shows the spatial distribution of the five fire classes. The class characteristics have been presented already. Class 1 fires are found predominantly at high latitudes (both North and South) and in temperate maritime regions. In boreal regions many fires are caused by lightning (Stocks, 1992), however, the density of fire activity is low. Much of this region is forested and given the very low population densities, fire is not used to any appreciable extent in land management. In temperate maritime regions fire activity is restricted by unfavourable weather conditions, with no extended dry period in which fires can occur. The other regions in which class 1 fire activity is seen are in the forested areas of Brazil and Africa. Tropical forest does not support any significant burning; the few fires seen are in openings or degraded forest or are used for burning already felled timber.

Class 2 fire activity occurs in the mid-latitudes, where the climate is warmer and there is a dry period sufficiently long to allow vegetation to dry. Much of the western United States is characterized by this fire class. During the Spring and Summer fire is used in forest management, but many fires can also be started unintentionally. An extensive fire belt stretches from the Black sea to lake Baikal in Eurasia. Burning is used for grassland management in this area but fires can also get out of control and spread into forested areas (Associated Press news report 1996).

Class 3 fire activity is seen in arid and semiarid areas, such as the horn of Africa, western India and the Australian interior. Here there is little vegetation and there are very long dry periods, therefore fire activity is low and those fires that take place are not necessarily restricted to a particular period of the year. Class 3 also occurs in subtropical maritime areas, such as the south-eastern United States and southern China. Here there is not a very well developed dry season, however, temperatures are high enough to dry vegetation relatively quickly, therefore allowing fire activity during short dry spells.

Class 4 fires are not restricted to any particular geographical or climatic zone. They are seen in boreal regions, where it is not uncommon to have extremely large fire events. In tropical areas, such large agglomerations of fire are associated with savanna burning, particularly in sparsely populated areas, where fires are not highly controlled (e.g. Northern Australia, Southern Sudan, Angola). Quite an extensive band of fire activity is seen in Brazil to the east of the Amazonian forest. Large fires are known to occur in the *cerrado* and in grazing lands in this region (Hlavka *et al*., 1996).

Class 5, which is characterized by a very high number of fires, is essentially confined to tropical regions, with most of the savanna in Africa dominated by this class. It is also seen in parts of southern Asia, north-east Brazil and the 'Top End' of Australia. In these areas the climate is characterized by high temperatures, large quantities of rainfall and a dry season from three to six months. These conditions are ideal for vegetation growth and its subsequent desiccation. Fire is used for a myriad of purposes in these ecosystems, e.g. grassland management, hunting, crop residue burning and land clearance (Andreae, 1992).

The Kyoto protocol on climate change (UNEP/IUC, 1998) makes specific reference to vegetation fire as a source of greenhouse gases. It furthermore requires signatories to the protocol to develop systematic observation systems and work to improve the quality of the data and methodologies used for estimating the emissions (Article 10). This study has shown the feasibility of providing objective and globally consistent information on vegetation fire using satellite observations and could potentially be used to help in making a first estimate of global greenhouse gas emissions due to vegetation fire very near in time to the baseline year of 1990.

In the tropics, especially in savanna, the fire return interval is very short, with the same area being burned year after year. The number of fires and the fire characteristics change in relation to climatic factors, however, regional patterns remain quite constant as has been observed in multiyear satellite data sets (Miranda *et al*., 1994; Koffi *et al*., 1996). In temperate and in boreal regions, although the number of fires may not vary greatly from year to year there is a very large interannual variation in the area burned (Stocks, 1992). Long-term monitoring of global fire occurrence with satellite data will allow us to improve characterization of fire regimes and aid our understanding of the complex relationship between climate, vegetation, land-use and fire. Although the analysis described here was restricted to a 12-month period, by lack of suitable long-term data sets, the results have demonstrated the feasibility of extracting useful information from such global data sets.

ACKNOWLEDGMENTS

E. Dwyer was funded by the TMR doctoral programme of the European Commission. Thanks to Michel Verstraete for his comments on the manuscript.

REFERENCES

Andreae, M.O. (1992) Biomass burning: its history, use, and distribution and its impact on environmental quality and global climate. *Global biomass burning, atmospheric, climatic, and biospheric implications* (ed. by J. Levine), pp. 3–21. MIT Press, Cambridge, Mass.

Cahoon, D. R., Stocks, B. J., Levine, J. S., Cofer, W. R. & O'Neill, K. P. (1992) Seasonal distribution of African savanna fire. *Nature,* **359**, 812–815.

Christensen, N.L. (1993) Fire regimes and ecosystem dynamics. *Fire in the environment* (ed. by P. J. Crutzen and J. G. Goldammer), pp. 233–244. Wiley and Sons, Chichester.

Crutzen, P.J. & Andreae, M.O. (1990) Biomass burning in the tropics: impact on atmospheric chemistry and biogeochemical cycles. *Science,* **250**, 1669–1788.

Davis, J.C. (1973) *Statistics and data analysis in geology.* Wiley & Sons, New York.

Davis, F. W., Quattrochi, D. A., Kidd, M. K., Lam, N. S.-N., Walsh, S. J., Michaelsen, J. C., Franklin, J., Stow, D. A., Johannsen, C. J. & Johnston, C. A. (1991) Environmental analysis using integrated GIS and remotely sensed data: some research needs and priorities. *Photogramm. Engng Remote Sensing,* **57**, 689–697.

DeFries, R., Hansen, M. & Townshend, J. (1995) Global discrimination of land cover types from metrics derived from AVHRR pathfinder data. *Remote Sensing Environ.* **54**, 209–222.

Delmas, R. A., Loudjani, P., Podaire, A. & Menaut, J.-C. (1992) Biomass burning in Africa: an assessment of annually burned biomass. *Global biomass burning* (ed. by J. Levine), pp. 126–132. MIT Press, Cambridge, Mass.

Dwyer, E., Grégoire, J.-M. & Malingreau, J. P. (1998) A global analysis of vegetation fires using satellite images: spatial and temporal dynamics. *Ambio,.* **27**, 175–181.

Eastman, J.R. & Fulk, M. (1993) Long sequence time series evaluation using standardized principal components. *Photogramm. Engng Remote Sensing,* **59**, 1307–1312.

Eva, H. & Lambin, H.&. (1998) Remote sensing of biomass burning in tropical regions: sampling issues and multisensor approach. *Remote Sensing Environ.* **64**, 292–315.

Eva, H. D., Malingreau, J. P., Grégoire, J.-M., Belward, A. S. & Mutlow, C. T. (1998) The advance of burnt areas in central Africa as detected by ERS-1 ATSR-1. *Int J. Remote Sensing,* **19**, 1635–1637.

Flasse, S. & Ceccato, P. (1996) A contextual algorithm for AVHRR fire detection. *Int J. Remote Sensing,* **17**, 419–424.

French, N. H. F., Kasischke, E. S., Johnson, R. D., Bourgeau-Chavez, L. L., Frick, A. L. & Ustin, S. (1996) Estimating fire-related carbon flux in Alaskan boreal forests using multisensor remote-sensing data. *Biomass burning and global change*, Vol. 2 (ed. by J. Levine), pp. 808–826. MIT Press, Cambridge, Mass.

Frulla, L. A., Milovich, J. A. & Gagliardini, D. A. (1995) Illumination and observation geometry for NOAA-AVHRR images. *Int J. Remote Sensing,* **16**, 2233–2253.

Fung, T. & LeDrew, E. (1987) Application of principal components analysis to change detection. *Photogramm. Engng Remote Sensing,* **53**, 1649–1658.

Giglio, L., Kendall, J. D. & Justice, C. O. (1999) Evaluation of global fire detection algorithms using simulated AVHRR infrared data. *Int J. Remote Sensing,* **20**, 1947–1985.

Goldammer, J.G. (1993) Historical biogeography of fire: tropical and subtropical. *Fire in the environment* (ed. by P. J. Crutzen and J. G. Goldammer), pp. 297–314. Wiley and Sons, Chichester.

Gonzalez, R.C. & Wintz, P. (1987) *Digital image processing*, 2nd edn, 503 pp. Addison-Wesley, Mass.

Grégoire, J.-M. (1993) Description quantitative des régimes de feu en zone soudanienne d'Afrique de l'Ouest. *Sécheresse,* **4**, 37–45.

Hao, W. & Liu, M. (1994) Spatial and temporal distribution of tropical biomass burning. *Global Biochem. Cycles,* **8**, 495–503.

Hlavka, C. A., Ambrosia, V. G., Brass, J. A., Rezendez, A. R. & Guild, L. S. (1996) Mapping fire scars in the Brazilian cerrado using AVHRR imagery. *Biomass burning and global change*, Vol. 2 (ed. by J. Levine), pp. 555–560. MIT Press, Cambridge, Mass.

IGBP (1992) *Improved global data for land applications, IGBP Global Change Report No. 20* (ed. by R. G. Townshend). IGBP, Stockholm and Toulouse.

IGBP (1994) IGBP-DIS satellite fire detection algorithm workshop technical report Working Paper 9. IGBP, Toulouse.

IGBP. (1997) Definition and implementation of a global fire product derived from AVHRR data. Working Paper 17. IGBP, Toulouse.

Johnston, R.J. (1978) *Multivariate statistical analysis in geography*, 280 pp. Longman, London.

Jones, S.H. (1997) Vegetation fire in mainland Southeat Asia: spatio-temporal analysis of AVHRR 1 km data for the 1992/93 dry season. Report no. EUR 17282 EN. European Commission, Luxembourg.

Keiner, L.E. & Yan, X.-H. (1997) Empirical orthogonal function analysis of sea surface temperature patterns in Delaware bay. *IEEE Trans. Geosci. Remote Sensing,* **35**, 13199–13206.

Kim, J.H. & Newchurch, M.J. (1998) Biomass-burning influence on tropospheric ozone over New Guinea and South America. *J. geophys Res.* **103,** 1455–1461.

Koffi, B., Grégoire, J.-M. & Eva, H. D. (1996) Satellite monitoring of vegetation fires on a multiannual basis at continental scale in Africa. *Biomass burning and global change*, Vol. 1 (ed. by J. Levine), pp. 225–235. MIT Press, Cambridge, Mass.

Levine, J.S. (1996) Introduction. *Biomass burning and global change*, Vol. 1 (ed. by J. Levine), pp. xxxv-xliii. MIT Press, Cambridge, Mass.

Lloyd, D. (1990) A phenological classification of terrestrial vegetation cover using shortwave vegetation index imagery. *Int J. Remote Sensing,* **11**, 2269–2279.

Malingreau, J.-P. & Grégoire, J.-M. (1996) Developing a global vegetation fire monitoring system for global change studies: a framework. *Biomass burning and global change*, Vol. 1 (ed. by J. Levine), pp. 14–24. MIT Press, Cambridge, Mass.

Menaut, J.-C., Abbadie, L. & Vitousek, P. M. (1993) Nutrient and organic matter dynamics in tropical ecosystems. *Fire in the environment: the ecological, atmospheric, and climatic importance of vegetation fires* (ed. by P. J. Crutzen and J. G. Goldammer), pp. 215–231. Wiley and Sons, Chichester.

de Miranda, E. E., Setzer, A. W. & Takeda, A. M. (1994) *Monitoramento Orbital das Queimadas No Brasil* (Remote sensing of fires in Brazil), 149 pp. ECOFORÇA, Campinas.

Piwowar, J.M. & LeDrew, E.F. (1996) Principal components analysis of Arctic ice conditions between 1978 and 1987 as observed from the SMMR data record. *Can J. Remote Sensing,* 22, 390–403.

Piwowar, J. M., Peddle, D. R. & LeDrew, E. F. (1998) Temporal mixture analysis of arctic sea ice imagery: a new approach for monitoring environmental change. *Remote Sensing Environ.* **63**, 195–207.

Richards, J.A. (1993) *Remote sensing digital image analysis*. Springer-Verlag, Berlin.

Robinson, J. (1991) Fire from space: global fire evaluation using infrared remote sensing. *Int J. Remote Sensing,* **12**, 3–24.

Singh, A. & Harrison, A. (1985) Standardized principal components. *Int J. Remote Sensing,* **6**, 883–896.

Stocks, B.J. (1992) The extent and impact of forest fires in northern circumpolar countries. *Global biomass burning, atmospheric, climatic, and biospheric implications* (ed. by J. Levine), pp. 197–202. MIT Press, Cambridge, Mass.

Stocks, B. J., Cahoon, D. R., Cofer, W. R. III & Levine, J. S. (1996) Monitoring large-scale forest-fire behavior in northeastern Siberia using NOAA-AVHRR satellite imagery. *Biomass burning and global change*, Vol. 2 (ed. by J. Levine), pp. 802–807. MIT Press, Cambridge, Mass.

Stroppiana, D., Pinnock, S. & Grégoire, J.-M. (1999) The global fire product: daily fire occurrence, from April 1992 to December 1993, derived from NOAA-AVHRR data. *Int J. Remote Sensing,* in press.

Townshend, J. R. G., Goff, T. E. & Tucker, C. J. (1985) Multi-temporal dimensionality of images of normalized difference vegetation index at continental scales. *IEEE Trans. Geosci. Remote Sensing,* **GE-23** 888–895.

Trabaud, L. V., Christensen, N. L. & Gill, A. M. (1993) Historical biogeography of fire in temperate and mediterranean ecosystems. *Fire in the environment* (ed. by P. J. Crutzen and J. G. Goldammer), pp. 277–296. Wiley and Sons, Chichester.

Tucker, C. J., Townshend, J. R. G. & Goff, T. E. (1985) African land-cover classification using satellite data. *Science,* **227,** 369–375.

UNEP/I. U. C. (1998) *The Kyoto Protocol to the Convention on Climate Change*, 34 pp. Climate Change Secretariat, Bonn and UNEP/IUC, Geneva.

Yarnal, B. (1993) *Synoptic climatology in environmental analysis*. Belhaven Press, London.

Zhuang, Y.-H., Cao, M., Wang, X. & Yao, H. (1996) Spatial distribution of trace-gas emissions from burning crop residue in China. *Biomass burning and global change*, Vol. 2 (ed. by J. Levine), pp. 764–770. MIT Press, Cambridge, Mass.

BIOSKETCHES

Edward Dwyer received an MSc in remote sensing from the University of Edinburgh. He is currently carrying out his PhD research using remotely sensed data to characterize global vegetation fire distributions and investigate the links between fire, climate and vegetation distributions.

José Miguel Pereira is an associate Professor. He obtained a PhD from the University of Arizona, in 1989. His main research interests are in the remote sensing of vegetation and fire activity, including burnt area mapping and estimation of atmospheric emissions from biomass burning.

Jean-Marie Grégoire obtained a PhD in 1980 from the Louis Pasteur University, Strasbourg on the use of remote sensing in the field of modelling of water and energy transfer in the soil-plant-atmosphere system. He is currently a project leader and his research interests are in developing remote sensing approaches to environmental monitoring and in particular fire.

Carlos C. DaCamara received a PhD degree in Atmospheric Sciences from the University of Missouri-Columbia (USA) in 1991. He is currently an Assistant Professor. His research has been partly devoted to exploring relationships between Atmospheric Circulation Types and wildfire activity.